Generation of mid-infrared pulses by $\chi^{(3)}$ difference frequency generation in CaF_2 and BaF_2

Han-Kwang Nienhuys

FOM Institute for Atomic and Molecular Physics, Kruislaan 407, 1098 SJ Amsterdam, The Netherlands

Paul C. M. Planken

Delft University of Technology, Faculty of Applied Sciences, Department of Applied Physics, Lorenztweg 1, 2628 CJ Delft, The Netherlands

Rutger A. van Santen

Schuit Catalysis Institute, Eindhoven University of Technology, P.O. Box 513, 5600 MB Eindhoven, The Netherlands

Huib J. Bakker

FOM Institute for Atomic and Molecular Physics, Kruislaan 407, 1098 SJ Amsterdam, The Netherlands

Received April 4, 2001

Tunable mid-IR pulses in the range 1300–4200 cm^{-1} (7.7–2.4 μm) are generated through a phase-matched four-wave mixing process in ordinary mid-IR window materials such as CaF_2 and BaF_2. In this process the difference frequency $\nu_3 = 2\nu_2 - \nu_1$ is generated from pump fields ν_1 and ν_2. The process can be phase matched to different frequencies by adjustment of the angle between the pump fields. © 2001 Optical Society of America

OCIS codes: 190.4380, 140.3070, 160.4330, 320.7110.

Mid-IR spectroscopy, which covers roughly the wavelength range 2.5–10 μm, has a long tradition as an analytical tool in chemistry, since molecular vibrations typically absorb in this wavelength range. However, linear mid-IR spectroscopy provides no information on processes on short time scales. The study of these processes requires time-resolved (or nonlinear) mid-IR spectroscopic techniques that employ high-intensity picosecond or femtosecond pulses. For example, in studies of the O–H stretch vibration in water[1,2] and the C–O vibration in organic molecules,[3,4] most dynamics (energy relaxation, molecular reorientation) occurs on a typical time scale of 1 ps.

The common methods for generating femtosecond mid-IR pulses employ various kinds of three-wave mixing processes, such as difference frequency generation[5,6] and optical parametric generation and (or) amplification (OPG/OPA).[7–9] Reference 10 is a review of several OPG/OPA methods. These processes all rely on the second-order polarization $P^{(2)}(t) \propto \chi^{(2)}E^2(t)$ created by a high-intensity field $E(t)$. This second-order polarization is nonzero only in materials that lack inversion symmetry. In such a system, fields with frequencies $\tilde{\nu}_1$ and $\tilde{\nu}_2$ couple to a field with frequency $\tilde{\nu}_3 = \tilde{\nu}_1 \pm \tilde{\nu}_2$. A high efficiency can be obtained only if the phase-matching condition $\mathbf{k}_3 = \mathbf{k}_1 \pm \mathbf{k}_2$ is fulfilled. The wave vectors $\mathbf{k}_x$ have magnitudes $k_x = \tilde{\nu}_x/n_x$, where n_x is the index of refraction at frequency $\tilde{\nu}_x$ (we use the wave number [in cm^{-1}] as a frequency quantity). Since in a medium with a normal dispersion, $n(\tilde{\nu})$ is a monotonically increasing function of $\tilde{\nu}$, the phase-matching condition can be satisfied only if the different fields have different polarizations, and the birefringence of the $\chi^{(2)}$ material is used, such that the $\tilde{\nu}_3$ field experiences a lower index of refraction than the $\tilde{\nu}_2$ field. Hence, to be suitable for $\chi^{(2)}$ IR generation a crystal should (1) be transparent for the wavelengths involved, (2) lack inversion symmetry, and (3) have the right amount of birefringence. Unfortunately, the available crystals for wavelengths beyond 4.5 μm, such as $AgGaS_2$,[6] GaSe,[5] and $ZnGeP_2$,[11] cannot be directly pumped with the currently available high-intensity 800-nm Ti:sapphire lasers.

As an alternative to the $\chi^{(2)}$-based pulse generation discussed above, we now consider $\chi^{(3)}$ (or four-wave mixing) processes. Here, three fields interact and drive a third-order polarization $P^{(3)}(t) \propto \chi^{(3)}E^3(t)$. Compared with $\chi^{(2)}$ processes, $\chi^{(3)}$ processes have the advantage that $\chi^{(3)}$ is nonzero in any medium, without any restrictions on the crystal symmetry. Therefore, $\chi^{(3)}$ frequency mixing is, in principle, possible in any medium, including isotropic media. Since such media have no birefringence, one must use alternative means to fulfill the requirement of phase matching.

Thus, pulses in various wavelength ranges have been generated. For example, far-IR (~60-cm^{-1}) pulses have been generated in air.[12] Because of the low value of $\chi^{(3)}$ in air, the pulse energy was only ~5 pJ, which required time-gated and phase-sensitive terahertz detection schemes. In the UV the properties of certain modes in hollow fibers have been employed to generate light in gases at well-chosen pressures with ~4-μJ pulse energies.[13] Further, in the mid IR, 1064-nm and tunable dye-laser pulses have been combined for generation of tunable picosecond

0146-9592/01/171350-03$15.00/0

pulses at ~1-pJ pulse energies in a phase-matched $\chi^{(3)}$ process.[14]

In this Letter we show how the approach reported in Ref. 14 can be used to generate mid-IR (2.4–7.6-μm) pulses with high energies and femtosecond durations with the currently available titanium sapphire laser systems. Here, pump fields with frequencies $\tilde{\nu}_1$ and $\tilde{\nu}_2$ generate a difference frequency $\tilde{\nu}_3 = 2\tilde{\nu}_2 - \tilde{\nu}_1$, with $\mathbf{k}_3 = 2\mathbf{k}_2 - \mathbf{k}_1$ as the phase-matching condition. We use the common window materials CaF_2 and BaF_2 as generating media. In these nonbirefringent materials, phase matching is possible, despite the fact that they have a normal dispersion, because this process uses the high-frequency field $2\tilde{\nu}_2$, with an index of refraction $n(\tilde{\nu}_2) < n(\tilde{\nu}_1)$.

For a pump frequency $\tilde{\nu}_1 = 12\,400$ cm^{-1} (806 nm), it turns out that collinear phase matching occurs at $\tilde{\nu}_3 = 2540$ cm^{-1} (3.9 μm) in CaF_2. Similarly, 7.8-μm light can be generated in BaF_2. Since these materials are not birefringent, rotating the crystal does not affect the wavelength at which the process is phase matched. However, the phase-matching can be tuned with the angle between the pump beams.

We used a commercial Ti:sapphire laser (Quantronix Titan; 100-fs, 2.5-mJ pulses, 1-kHz repetition rate) to pump a β-barium borate optical parametric conversion stage (Light Conversion Topas). From the output of the parametric conversion stage, we used the signal (6250–8300 cm^{-1}, 300 μJ) and the remaining pump (12 400 cm^{-1}, 1.1 mJ) for the $\tilde{\nu}_2$ and $\tilde{\nu}_1$ fields, respectively, as shown in Fig. 1. After being split and recombined for time overlap, the pulses were collimated to an approximately 2-mm diameter before interacting in a 4-mm CaF_2 or BaF_2 plate. Because of the properties of the $\chi^{(3)}$ tensor, the intensity of the generated $\tilde{\nu}_3$ field is a factor of 9 higher for parallel $\tilde{\nu}_1$ and $\tilde{\nu}_2$ pump fields than for perpendicular pump fields.[15] Therefore, we used a wave plate to make the polarizations of the pump and signal pulses parallel.

A delay stage permitted adjustment of the time overlap between the pump and signal pulses. At time overlap, we generated pulses with typical energies of 100–200 nJ.

If the laser pulses are focused in air in a collinear geometry, similar to Ref. 12, a measurable amount of IR is generated as well but with a typical energy of only 3 nJ and a bandwidth of 400 cm^{-1} FWHM. Also, a visible amount of light at frequency $2\tilde{\nu}_1 - \tilde{\nu}_2$ is generated in this case.

Figure 2 shows the tuning curve with the generated frequency, $\tilde{\nu}_3$, versus the angle $\beta = \angle(\mathbf{k}_1, \mathbf{k}_3)$. Calculated tuning curves are shown as well; we obtain these by substituting $k_x = n_x\tilde{\nu}_x$ in the phase-matching condition $\mathbf{k}_3 = 2\mathbf{k}_2 - \mathbf{k}_1$, which yields

$$\cos(\beta) = \frac{4n_2{}^2\tilde{\nu}_2{}^2 - n_1{}^2\tilde{\nu}_1{}^2 - n_3{}^2\tilde{\nu}_3{}^2}{2n_1n_3\tilde{\nu}_1\tilde{\nu}_3}, \qquad (1)$$

where n_i are the indices of refraction as calculated from the Sellmeier equations for CaF_2 (Refs. 16 and 17) and BaF_2.[16,18]

For BaF_2, we obtained better agreement between the experiment and the calculated tuning curve if we increased the index of refraction at frequency $\tilde{\nu}_1$ by 1.0×10^{-4}. Instead of 1286 cm^{-1} (7.8 μm) and 6.5° for the cutoff frequency and maximum angle, respectively, n_2 yields 1325 cm^{-1} and 6.0°, respectively (as shown in Fig. 2). In CaF_2, the difference between experiment and theory can result from a frequency-dependent deviation of less than 10^{-4} in the refractive index for the $\tilde{\nu}_2$ field. We note that the experimental values of the index of refraction are known to differ by similar amounts from the calculated values.[16–18]

Figure 3 shows typical spectra of the pulses generated in CaF_2 and BaF_2. We obtained these spectra with a scanning monochromator and PbSe (for the CaF_2 data) and HgCdTe (for BaF_2) detectors. We chose these detectors for their different spectral responses. To tune $\tilde{\nu}_3$, we adjusted both $\tilde{\nu}_2$ (which defines the difference frequency $\tilde{\nu}_3$) and the angle between $\mathbf{k}_1$ and $\mathbf{k}_2$ (phase matching). The FWHM bandwidth of the generated spectra is ~200 cm^{-1} for CaF_2 and 40–300 cm^{-1} for BaF_2, respectively. The maximum frequency $\tilde{\nu}_3$ is approximately 4100 cm^{-1}, limited by $\tilde{\nu}_2$, which could not be tuned higher than ~8250 cm^{-1} in our OPG/OPA.

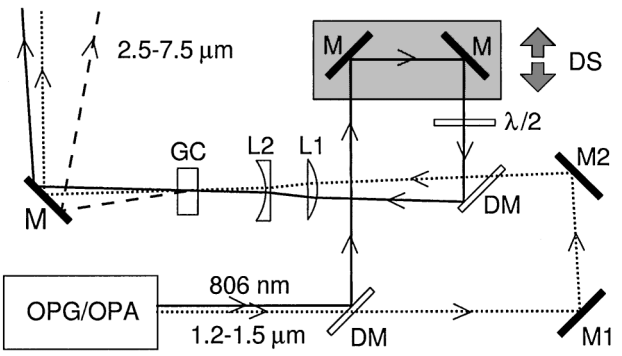

Fig. 1. Setup for $\chi^{(3)}$ pulse generation. DMs, dichroic mirrors; M, M1, M2, mirrors; $\lambda/2$, half-wave plate; DS, delay stage; L1, L2, 2:1 telescope (BK7 glass); GC, generation crystal (4-mm CaF_2 or BaF_2). We used M1 and M2 to adjust the angle between the pump and the signal beams.

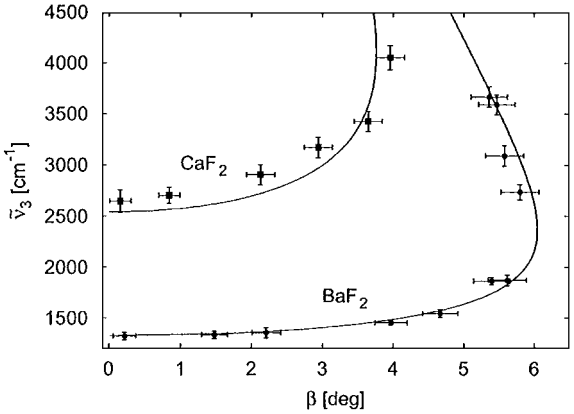

Fig. 2. Tuning curves for BaF_2 and CaF_2. Data points, experimental values, with the FWHM bandwidth as the vertical error bar. Curves, calculated tuning curves for $\tilde{\nu}_1 = 12\,400$ cm^{-1}.

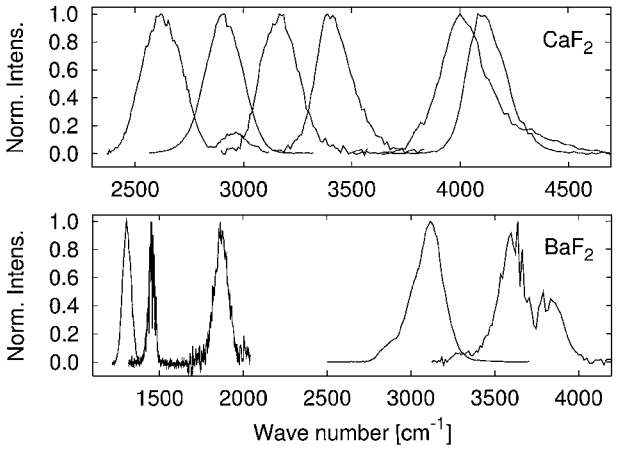

Fig. 3. Typical spectra of the generated pulses in CaF_2 and BaF_2. The structure in the spectra at 1500 and 3700 cm^{-1} is caused by absorption lines of water vapor.

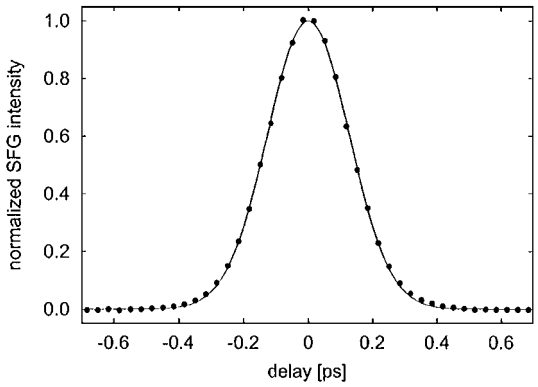

Fig. 4. Autocorrelate of pulses generated in CaF_2 at 2580 cm^{-1} with a fit to a Gaussian pulse shape. SFG, sum frequency generation.

Figure 4 shows an autocorrelate for pulses generated in CaF_2 at 2580 cm^{-1}. We measured this by generating the second harmonic of the IR pulses in a $LiIO_4$ ($\theta = 20°$) crystal. The FWHM autocorrelate width is 298 fs, which corresponds to a 211-fs pulses duration if we assume a Gaussian pulse shape. With a 200-cm^{-1} FWHM bandwidth, this yields $\Delta\nu\Delta\tau = 1.3$ for the frequency–bandwidth product.

To summarize, we have shown that a $\chi^{(3)}$ difference frequency generation process with two pump fields can be phase matched in the common IR window materials CaF_2 and BaF_2, which have no special birefringent or crystal symmetry properties. An 806-nm laser pulse as the high-frequency ($\tilde{\nu}_1$) pump permits generation of difference frequencies over the range 2.4–7.6 μm with the angle between the pumping fields as a tuning parameter. We obtained pulse energies of up to 200 nJ.

As a final note we point out that the presented type of $\chi^{(3)}$ difference frequency generation can be phase matched in any material with a normal dispersion relation, although the angles and cutoff wavelengths vary. A common material especially worth mentioning in this respect is NaCl, with $\tilde{\nu}_3 > 600$ cm^{-1} and $\beta < 17°$.

This work is part of a collaborative research program of NIOK (Netherlands Graduate School of Catalysis Research) and FOM (Foundation for Fundamental Research on Matter), which is financially supported by NWO (Netherlands Organization for the Advancement of Research). H.-K. Nienhuys's e-mail address is h.nienhuys@amolf.nl.

References

1. H. K. Nienhuys, R. A. van Santen, and H. J. Baker, J. Chem. Phys. **112,** 8487 (2000).
2. G. M. Gale, G. Gallot, F. Hache, N. Lascoux, S. Bratos, and J.-C. Leickman, Phys. Rev. Lett. **82,** 1068 (1999).
3. C. Chudoba, E. T. J. Nibbering, and T. Elsaesser, Phys. Rev. Lett. **81,** 3010 (1998).
4. P. Hamm, M. Lim, and R. M. Hochstrasser, J. Phys. Chem. B **102,** 6123 (1998).
5. R. A. Kaindl, M. Wurm, K. Reimann, P. Hamm, A. M. Weiner, and M. Woerner, J. Opt. Soc. Am. B **17,** 2086 (2000).
6. P. Hamm, C. Lauterwasser, and W. Zinth, Opt. Lett. **18,** 1943 (1993).
7. V. Petrov and F. Noack, J. Opt. Soc. Am. B **12,** 2214 (1995).
8. G. M. Gale, G. Gallot, F. Hache, and R. Sander, Opt. Lett. **22,** 1253 (1997).
9. U. Emmerichs, S. Woutersen, and H. J. Bakker, J. Opt. Soc. Am. B **14,** 1480 (1997).
10. M. H. Dunn and M. Ebrahimzadeh, Science **286,** 1513 (1999).
11. V. Petrov, F. Rotermund, F. Noack, and P. Schunemann, Opt. Lett. **24,** 414 (1999).
12. D. J. Cook and R. M. Hochstrasser, Opt. Lett. **25,** 1210 (2000).
13. C. G. Durfee, S. Backus, M. M. Murnane, and H. C. Kapteyn, Opt. Lett. **22,** 1565 (1997).
14. H. Okamoto and M. Tasumi, Opt. Commun. **121,** 63 (1995).
15. Y. R. Shen, *The Principles of Nonlinear Optics* (Wiley, New York, 1984).
16. P. I. Klocek, ed., *Handbook of Infrared Optical Materials* (Marcel Dekker, New York, 1991).
17. I. H. Malitson, Appl. Opt. **2,** 1103 (1963).
18. I. H. Malitson, J. Opt. Soc. Am. **54,** 628 (1964).